INTERNATIONAL JOURNAL FOR NUMERICAL METHODS IN ENGINEERING
Int. J. Numer. Meth. Engng. **44**, 229–248 (1999)

NEW ENHANCED STRAIN ELEMENTS FOR INCOMPRESSIBLE PROBLEMS

J. M. A. CÉSAR DE SÁ* AND R. M. NATAL JORGE

Department of Mechanical Engineering, Faculty of Engineering, University of Porto, Portugal

ABSTRACT

A new enhanced strain element, based on the definition of extra compatibles modes of deformation added to the standard four-node finite element, is initially presented. The element is built with the objective of addressing incompressible problems and avoiding locking effects. By analysing at the element level the deformation modes which form a basis for the incompressible subspace the extra modes of deformation are proposed in order to provide the maximum possible dimension to that subspace. Subsequently another new element with more degrees of freedom is formulated using a mixed method. This is done by including an extra field of variables related to the derivatives of the displacement field of the extra compatible modes defined previously. The performance of the elements proposed is assessed in linear and non-linear situations.

KEY WORDS: incompressibility; enhanced strain; mixed methods

1. INTRODUCTION

The improvement of the performance of low-order quadrilateral elements, namely in the presence of incompressible deformations, have been, in the recent years, an important issue of discussion, despite the fact that some good solutions are already available and adopted in many general purpose finite element programs. The main reason lies in the fact that low-order elements are preferred in large-scale computations, involving very often adaptive mesh refinements, which are very often associated to the solution of practical engineering problems, as those encountered in metal-forming applications.

Nevertheless, incompressible or near incompressible behaviour has been a source of problems for finite element analysis with low-order elements as they tend to present a locking response on those conditions. In different fields as linear and non-linear elasticity, viscous incompressible fluid flow or plastic deformation those problems were early detected.[1–4]

* Correspondence to: J. M. A. César de Sá, Department of Mechanical Engineering, Faculty of Engineering, University of Porto, Rua dos Bragas, 4099 Porto Codex, Portugal. E-mail: cesarsa@fe.up.pt

Contract/grant sponsor: Programa PRAXIS XXI do Ministério da Ciência e Tecnologia do FEDER; Contract/grant number: 3/3.1/CEG/2643/95

CCC 0029–5981/99/020229–20$17.50

Received 27 October 1997
Revised 7 April 1998

Mixed formulations, based on sound mathematical grounds, when properly implemented, solved the problem with the disadvantage of introducing more variables. Reduced and selective reduced integration techniques, although initially taken as useful tricks, were the first irreducible form solutions for locking problems. Later Malkus and Hughes[5] established the equivalence of mixed formulations and selective reduced integration techniques of penalty formulations, under certain conditions. Later the **B**-bar method was introduced[6,7] which avoided the necessity of reduced integration and in which the shape function derivatives related to the volumetric response were replaced by approximations resulting from a mixed formulation. Some heuristic methods were even established in order to determine the ability of an element to perform well, based on the definition of a constraint ratio.[6–8] Alternative solutions were also obtained with the so-called incompatible modes of deformation introduced initially for bending,[9,10] that also behaved well in incompressible problems. Other routes exploiting the ideas of developing a stabilization matrix orthogonal to linear displacement fields to achieve flexural super-convergent solutions for the incompatible mode elements,[11] by introducing the so called γ-projection operator were also developed.[12]

César de Sá and Owen[13,14] analysed, at the element level, the subspace of incompressible deformation that result from the finite element solution and made clear how, under certain circumstances, the locking occurs. It was also shown that the constraint ratios may give wrong indications to evaluate a possible locking condition.

Simo and Rifai[15] introduced the concept of enhanced strain element built from an initial three field mixed formulation. The enhanced strain field is associated with variables that can be eliminated at element level. With this approach locking is avoided and good accuracy is achieved even with coarse meshes. They also defined the conditions on which this approach should be built and how it could include the method of incompatible modes. The element proved to behave well even for inelastic materials and later the concept was extended for geometrically non-linear and 3D finite deformation problems.[16,17]

Other contributions in the development and application of the enhanced strain concept can be found in more recent works.[18–21] However, de Souza Neto *et al.*[21] showed that, despite the benefits introduced by the enhanced strain element, when solving practical elastic and elastoplastic problems having particularly highly strained compressive regimes, some spurious hourglass patterns may develop.

A new simple low-order element was therefore proposed by de Souza Neto *et al.*[22] in which a multiplicative split of the deformation gradient into deviatoric and volumetric contributions is performed. These contributions are evaluated at the Gauss points and at the centroid similarly to the **B**-bar method. This element showed good behaviour in problems involving nearly incompressible hyperelasticity and finite multiplicative plasticity and also the ability to capture strain localisation phenomena.

Another interesting approach was presented by Wriggers and Hueck in References 23 and 24, unifying the concepts of incompatible modes and stabilisation.

In this paper the analysis of the subspace of incompressible deformation associated to the standard four-node element and developed by César de Sá and Owen[13,14] is reviewed and utilized to explain the success of some of the different elements proposed. Based on this insight into the locking phenomenon and using similar frameworks to the incompatible modes element and Simo and Rifai's enhanced strain element new elements for incompressible problems are proposed. These elements are based on extra compatible modes of deformation and its robustness in dealing with incompressible problems is assessed.

2. INCOMPRESSIBILITY AND LOCKING

The incompressible problem may be stated as a constrained minimization of a functional. In simple terms, we want to obtain, in the linear space of admissible solutions U, the displacement field $\mathbf{u}$ that minimizes the total energy of the system, with the restriction of belonging to a subspace of U, which we may name as the subspace of incompressible deformations $I \subset U$.

Using the Lagrange multiplier method the problem is transformed into the minimization of the unconstrained augmented functional:

$$\pi(\mathbf{u}, \lambda) = \int_\Omega \frac{1}{2}\mathbf{s} : \boldsymbol{\varepsilon}\, d\Omega - \int_\Omega \mathbf{b}\cdot\mathbf{u}\, d\Omega - \int_{\Gamma_\sigma} \mathbf{t}\cdot\mathbf{u}\, d\Gamma - \int_\Omega \lambda\, \mathrm{div}(\mathbf{u})\, d\Omega \tag{1}$$

in which $\mathbf{s}$ is the deviatoric stress tensor, $\boldsymbol{\varepsilon}$ is the deviatoric strain tensor, $\mathbf{b}$ and $\mathbf{t}$ are the body force and surface traction vector functions and the Lagrange multiplier λ may be identified with the hydrostatic pressure p.

When a finite element solution is established the spaces U and I are approximated by finite dimensional spaces U^h and I^h. The two field finite element solution, given by the variational principle associated with equation (1), is obtained by

$$\begin{bmatrix} \mathbf{K} & \mathbf{Q}^{\mathrm{T}} \\ \mathbf{Q} & \mathbf{0} \end{bmatrix} \begin{bmatrix} \mathbf{u}^h \\ \mathbf{p}^h \end{bmatrix} = \begin{bmatrix} \mathbf{f}^h \\ \mathbf{0} \end{bmatrix} \tag{2}$$

in which $\mathbf{f}^h$ is the vector of applied forces and $\mathbf{K}$ is the deviatoric stiffness matrix.

The incompressible constraint, that is obtained from the variation of the functional on p, is represented by the second set of equations on (2)

$$\mathbf{Q}\mathbf{u}^h = \mathbf{0} \tag{3}$$

and defines the subspace of incompressible deformations I^h as

$$I^h = \{\mathbf{u}^h \in U^h : \mathbf{Q}\mathbf{u}^h = \mathbf{0}\} \tag{4}$$

The solution $\mathbf{u}^h$ should then lie on the null space of $\mathbf{Q}$, i.e. in the subspace of incompressible deformations I^h, and therefore be a linear combination of the elements of a given basis of I^h. But I^h is a finite-dimensional approximation space to I and therefore may not be able to reproduce all the possible solutions. Locking occurs when, for a given set of boundary conditions, the expected solution does not belong to I^h.[13,14] In this case the solution is whether the trivial one to equation (3), i.e. $\mathbf{u}^h = \mathbf{0}$ or only a linear combination of the components of a projection of the 'exact' solution on I^h, which may be a crude approximation. Different elements, for a given mesh, will

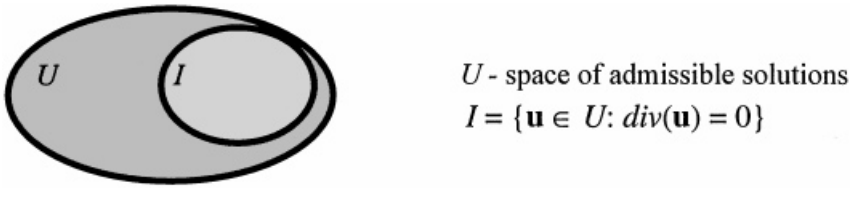

Figure 1. Space of admissible solutions and subspace of incompressible deformations

offer different approximations to the subspace of incompressible deformations and therefore different abilities to reproduce these type of situations.

3. BASES FOR THE SUBSPACE OF INCOMPRESSIBLE DEFORMATIONS

On the assumption of the equivalence theorem of Malkus and Hughes,[5] a clear illustration of the last statements was given by César de Sá and Owen[13,14] by showing, for the cases of a single linear element, with full and selective reduced integration, the mechanism of locking, in the context of infinitesimal strains. A brief summary of some results for a 2-D situation on ξ–η co-ordinates is recalled next and summarized in Figures 2 and 3.

In order to characterize I^h a basis was determined by imposing the incompressible constraint at each Gauss point. For the full integration case I^h is a subspace of dimension five determined by the equation

$$\varepsilon^h_{kk} = \left[\frac{\partial N_i}{\partial \xi} \quad \frac{\partial N_i}{\partial \eta}\bigg|_{i=1,n^e_{\text{nodes}}} \right] \mathbf{u}^h = \mathbf{0} \tag{5}$$

or

$$\begin{Bmatrix} \varepsilon^h_{kk}(\xi_1,\eta_1) \\ \varepsilon^h_{kk}(\xi_2,\eta_2) \\ \varepsilon^h_{kk}(\xi_3,\eta_3) \\ \varepsilon^h_{kk}(\xi_4,\eta_4) \end{Bmatrix} = \begin{bmatrix} -a_1 & -a_1 & a_1 & -a_2 & a_2 & a_2 & -a_2 & a_1 \\ -a_2 & -a_1 & a_2 & -a_2 & a_1 & a_2 & -a_1 & a_1 \\ -a_1 & -a_2 & a_1 & -a_1 & a_2 & a_1 & -a_2 & a_2 \\ -a_2 & -a_2 & a_2 & -a_1 & a_1 & a_1 & -a_1 & a_2 \end{bmatrix} \{\mathbf{d}_e\} = \mathbf{0} \tag{6}$$

where

$$a_1 = \tfrac{1}{4}(1 + a_0), \quad a_2 = \tfrac{1}{4}(1 - a_0) \quad \text{and} \quad a_0 = |\xi_i| = \frac{1}{\sqrt{3}} \tag{7}$$

and

$$\text{rank}(\mathbf{Q}) = 3 \wedge \text{nullity}(\mathbf{Q}) = 5 \tag{8}$$

For the selective reduced integration equation (5) defines I^h as a subspace of dimension seven, which is the maximum allowed as the dimension of the space of all admissible solutions is eight, and may be written as

$$\varepsilon^h_{kk}(\xi_0,\eta_0) = \tfrac{1}{4}[-1 \quad -1 \quad 1 \quad -1 \quad 1 \quad 1 \quad -1 \quad 1]\{\mathbf{d}_e\} = 0 \tag{9}$$

In this case we have

$$\text{rank}(\mathbf{Q}) = 1 \wedge \text{nullity}(\mathbf{Q}) = 7 \tag{10}$$

The comparison between two possible bases for those spaces, represented in Figure 2, shows clearly that the vectors on the basis of the full integration solution do not span the extra vectors of the basis of the selective reduced solution, b_6 and b_7. Therefore, any attempt to obtain those deformation patterns by conditioning the boundary conditions and applied forces results inevitably in a locking situation, as is presented in Figure 3. The same would happen, for full integration, in any other case in which the expected deformation field would have important components in these two extra basis vectors.

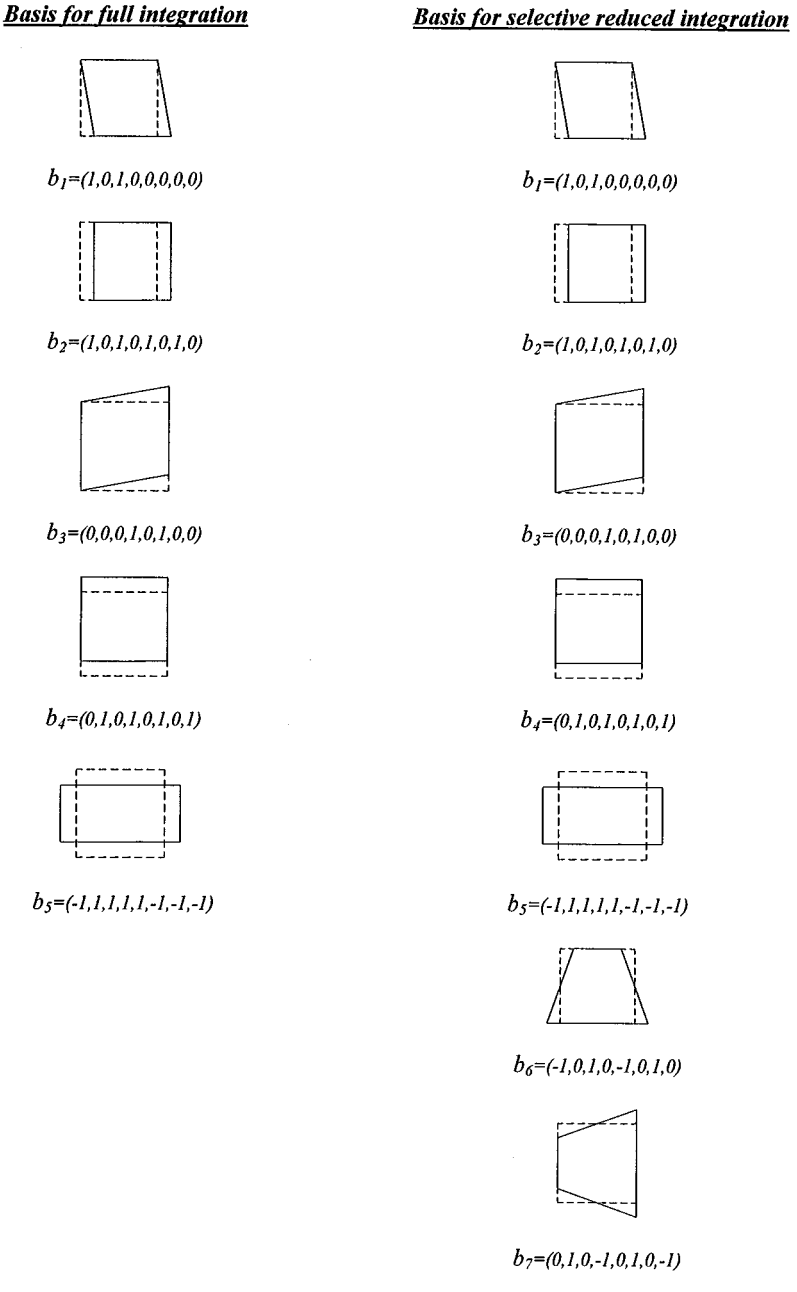

Figure 2. Basis for the incompressible deformation subspace (one element mesh)

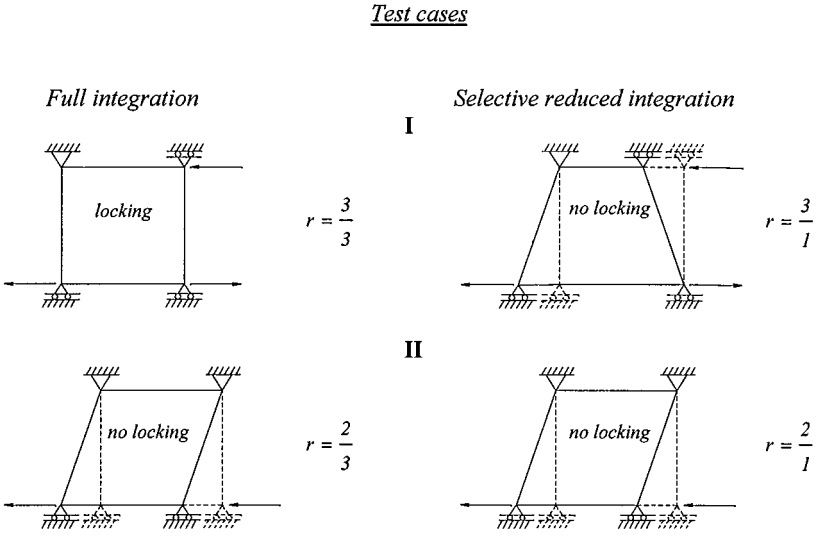

Figure 3. Tests: I—locking test; II—no locking test. Constraint ratio: r

In Figure 3 is also recalled[13,14] how the constraint ratio r defined in Reference 7 may give wrong indications of possible locking situations.

4. NEW ELEMENTS FOR INCOMPRESSIBILITY

It is interesting to see that if I^h is defined in the same manner for the different solutions to locking referred, namely the incompatible modes element, the **B**-bar element or the enhanced strain element the result is similar to that in the element with selective reduced integration, i.e. a similar seven-dimensional subspace is obtained, despite the fact that they are formulated in different ways. Bearing that in mind, we will try to formulate some new elements designed to deal with incompressibility, for 2-D problems, by assuming that the two extra modes of deformation, b_6 and b_7, should be reproducible.

4.1. The Qi5 element

This new element will be built by adding two extra compatible modes of deformation in the definition of the displacement field using the same framework as in the definition of the incompatible modes element. However, in this case, the Jacobian matrix does not have to be evaluated at the centre of the element, as we will see later.

In order to illustrate the methodology followed let us recover the locking test in Figure 3 and suppose that is possible to obtain the displacement field represented in Figure 4. If the displacement field is only defined from the standard expansion in terms of bilinear shape functions the divergence of the displacement field is never equal to zero at the Gauss points, as shown in Figure 4.

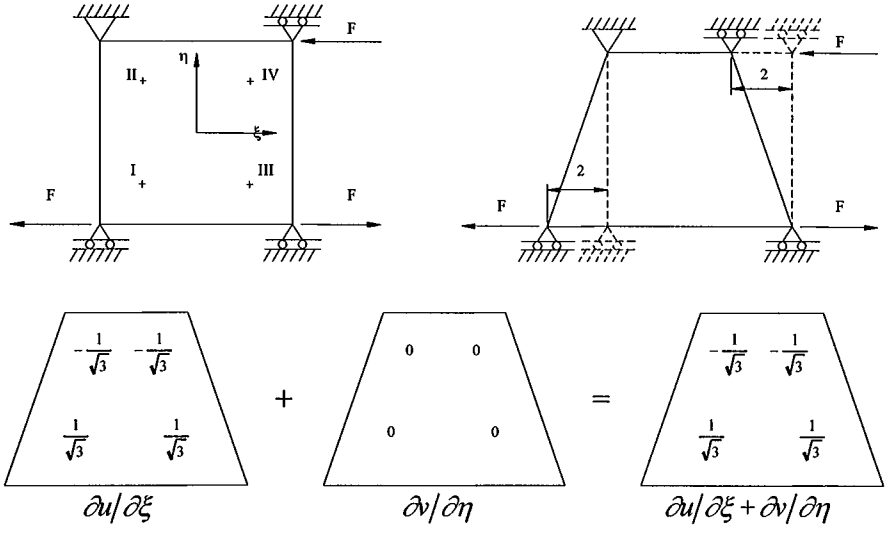

Figure 4. Locking test. Div($\mathbf{u}^h$) at the Gauss points of the b_6 mode of deformation with full integration

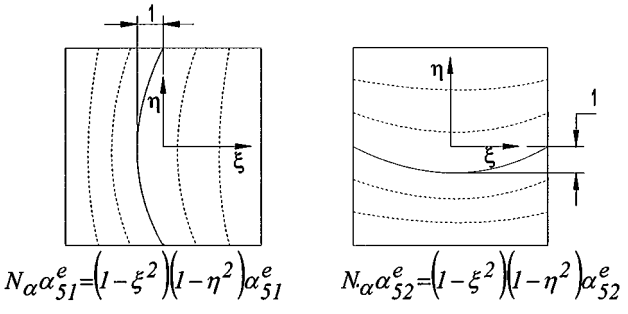

Figure 5. Additional compatible modes

Therefore, the extra modes to be included should provide the possibility of div($\mathbf{u}$) be equal to zero at the Gauss points in an incompressible situation. This can be achieved by considering the extra compatible displacement field $\mathbf{u}^h_\alpha$, so that, at the element level (Figure 5):

$$\mathbf{u}^h = \mathbf{u}^h_d + \mathbf{u}^h_\alpha = \sum_{i=1}^{4} N_i(\xi,\eta)\mathbf{d}^e_i + N_\alpha(\xi,\eta)\alpha^e \tag{11}$$

with

$$\mathbf{d}^e_i = \begin{bmatrix} u^e_i \\ v^e_i \end{bmatrix}, \quad \alpha^e = \begin{bmatrix} \alpha^e_{51} \\ \alpha^e_{52} \end{bmatrix} \tag{12}$$

and

$$N_\alpha = (1-\xi^2)(1-\eta^2) \tag{13}$$

These extra compatible displacement field consist on an internal movement leaving the displacement at the element sides equal to zero and the components of α^e may be viewed as internal variables which may be associated to displacements of the central point. However, as in the case of incompatible modes element, their contribution should not be considered when evaluating the element body force vectors. It is interesting to note that this methodology leads to a similar procedure developed by Dvorkin and Vassolo.[25]

These extra modes of deformation allow the divergence of the displacement field to equal zero at the Gauss points for adequate values of the components of α^e. Their contribution for the div($\mathbf{u}^h$), in local co-ordinates, is

$$\frac{\partial u_\alpha}{\partial \xi}\alpha^e_{51} + \frac{\partial v_\alpha}{\partial \eta}\alpha^e_{52} = -2\xi(1-\eta^2)\alpha^e_{51} - 2\eta(1-\xi^2)\alpha^e_{52} \tag{14}$$

In the locking test of Figure 4 if we assign the following values to the new variables:

$$\alpha^e_{51} = 0 \wedge \alpha^e_{52} = -\tfrac{3}{4} \tag{15}$$

then $\nabla \cdot \mathbf{u}^h = 0$ at the Gauss points, as it is illustrated in Figure 6.

Following the f.e.m. standard methodology then we may define

$$\varepsilon = \varepsilon_d + \varepsilon_\alpha = [\mathbf{B}^e_d \ \mathbf{B}^e_\alpha]\begin{bmatrix}\mathbf{d}^e \\ \alpha^e\end{bmatrix} \tag{16}$$

$$\mathbf{B}^e_d = \begin{bmatrix} \dfrac{\partial N_i}{\partial x} & 0 \\ 0 & \dfrac{\partial N_i}{\partial y} \\ \dfrac{\partial N_i}{\partial y} & \dfrac{\partial N_i}{\partial x} \end{bmatrix}_{i=1,4}, \quad \mathbf{B}^e_\alpha = \begin{bmatrix} \dfrac{\partial N_\alpha}{\partial x} & 0 \\ 0 & \dfrac{\partial N_\alpha}{\partial y} \\ \dfrac{\partial N_\alpha}{\partial y} & \dfrac{\partial N_\alpha}{\partial x} \end{bmatrix} \tag{17}$$

Taking in account the following relations:

$$\frac{\partial N}{\partial \mathbf{x}} = \begin{bmatrix} \dfrac{\partial N}{\partial x} \\ \dfrac{\partial N}{\partial y} \end{bmatrix} = \begin{bmatrix} \dfrac{\partial \xi}{\partial x} & \dfrac{\partial \eta}{\partial x} \\ \dfrac{\partial \xi}{\partial y} & \dfrac{\partial \eta}{\partial y} \end{bmatrix} \begin{bmatrix} \dfrac{\partial N}{\partial \xi} \\ \dfrac{\partial N}{\partial \eta} \end{bmatrix} = \mathbf{J}^{-\mathrm{T}}_{x,\xi}\frac{\partial N}{\partial \xi} \tag{18}$$

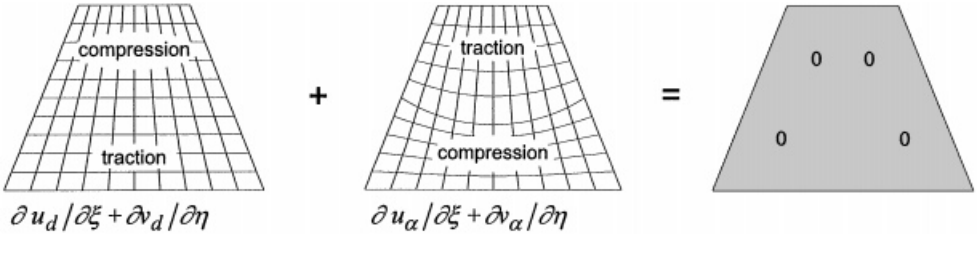

Figure 6. Locking test with additional degrees of freedom

$$\mathbf{J}_{x,\xi}^{-\mathrm{T}} = \frac{1}{j}\begin{bmatrix} \dfrac{\partial y}{\partial \eta} & -\dfrac{\partial y}{\partial \xi} \\ -\dfrac{\partial x}{\partial \eta} & \dfrac{\partial x}{\partial \xi} \end{bmatrix}, \quad j = |\mathbf{J}_{x,\xi}| = \frac{\partial x}{\partial \xi}\frac{\partial y}{\partial \eta} - \frac{\partial x}{\partial \eta}\frac{\partial y}{\partial \xi} \tag{19}$$

then $\mathbf{B}_\alpha^e$ takes the form

$$\mathbf{B}_\alpha^e = \begin{bmatrix} B_{\alpha 1} & 0 \\ 0 & B_{\alpha 2} \\ B_{\alpha 2} & B_{\alpha 1} \end{bmatrix} \tag{20}$$

in which

$$B_{\alpha 1} = \frac{\partial N_\alpha}{\partial x} = \frac{\partial N_\alpha}{\partial \xi}\frac{\partial \xi}{\partial x} + \frac{\partial N_\alpha}{\partial \eta}\frac{\partial \eta}{\partial x} = -2\xi(1-\eta^2)\frac{1}{j}\sum_{i=1}^{4}\frac{\partial N_i}{\partial \eta}y_i + 2\eta(1-\xi^2)\frac{1}{j}\sum_{i=1}^{4}\frac{\partial N_i}{\partial \xi}y_i \tag{21}$$

$$B_{\alpha 2} = \frac{\partial N_\alpha}{\partial y} = \frac{\partial N_\alpha}{\partial \xi}\frac{\partial \xi}{\partial y} + \frac{\partial N_\alpha}{\partial \eta}\frac{\partial \eta}{\partial y} = +2\xi(1-\eta^2)\frac{1}{j}\sum_{i=1}^{4}\frac{\partial N_i}{\partial \eta}x_i - 2\eta(1-\xi^2)\frac{1}{j}\sum_{i=1}^{4}\frac{\partial N_i}{\partial \xi}x_i \tag{22}$$

It is interesting to note that this element passes the patch test for arbitrary configurations with no need of referring the inverse of the Jacobian to the central point of the element, as in the cases of the incompatible modes or the enhanced strain elements. This is due to the fact that, in this case, the following relation:

$$\int_\Omega \mathbf{B}_\alpha \,\mathrm{d}\Omega = \int_{-1}^{1}\int_{-1}^{1} \mathbf{B}_\alpha \, j \,\mathrm{d}\xi \,\mathrm{d}\eta = \mathbf{0} \tag{23}$$

is satisfied,[7,10] which is not case for incompatible modes or the enhanced strain elements.

In Section 5 this element is assessed on various examples. As it will be shown it does not lock but its performance may not be as good as the enhanced strain element in bending dominated problems or in extreme incompressible conditions. This fact is not unexpected as the advantage of the Qi5 element of having less degrees of freedom than the QM6 may, otherwise, mean less ability to model those stringe conditions in non regular meshes. Therefore a new element based on the Qi5, but with more degrees of freedom will be developed in the next section.

4.2. The Qi6 element

This element designed is inspired in the works of Simo and Rifai[15] and Simo and Armero[16] and will be based on the Qi5 element developed in the previous section.

The crucial idea here is to include, via a mixed formulation, an extra field of variables related to the space derivatives of the displacement field. Thus, the actual displacement gradient matrix $\mathbf{H}$, is obtained by adding to the compatible part of the Jacobian matrix of the displacement field $\mathbf{J}_{\mathbf{u},\mathbf{x}}$ an enhanced part $\mathbf{J}_{\tilde{\mathbf{u}},\mathbf{x}}$ as follows:

$$\mathbf{H} = \mathbf{J}_{\mathbf{u},\mathbf{x}} + \mathbf{J}_{\tilde{\mathbf{u}},\mathbf{x}} \tag{24}$$

Therefore the actual deformation gradient $\mathbf{F}_\mathbf{a}$ is obtained from the compatible one $\mathbf{F}$ as

$$\mathbf{F}_\mathbf{a} = \mathbf{F} + \mathbf{J}_{\tilde{\mathbf{u}},\mathbf{x}} = \mathbf{I} + \mathbf{J}_{\mathbf{u},\mathbf{x}} + \mathbf{J}_{\tilde{\mathbf{u}},\mathbf{x}} \tag{25}$$

For a 2-D problem equation (24) reads:

$$\mathbf{H} = \begin{bmatrix} \dfrac{\partial u}{\partial x} & \dfrac{\partial u}{\partial y} \\ \dfrac{\partial v}{\partial x} & \dfrac{\partial v}{\partial y} \end{bmatrix} + \begin{bmatrix} \dfrac{\partial \tilde{u}}{\partial x} & \dfrac{\partial \tilde{u}}{\partial y} \\ \dfrac{\partial \tilde{v}}{\partial x} & \dfrac{\partial \tilde{v}}{\partial y} \end{bmatrix} \tag{26}$$

For a mixed finite element solution four extra α_{ij}^e variables, associated to this new field, are added to each element to obtain the terms in $\mathbf{J}_{\tilde{\mathbf{u}},\mathbf{x}}$. In order to satisfy the constant nominal stress field condition, which is closely related to the satisfaction of the classical patch test,[15,16] without having to scale the Jacobian matrix from centroid of the element to the Gauss points, the same derivatives of the shape function defined for the Qi5 element are used to represent the terms of the enhanced displacement gradient, as follows:

$$\frac{\partial \tilde{u}}{\partial x} = \frac{\partial N_\alpha}{\partial x}\alpha_{51}^e, \quad \frac{\partial \tilde{u}}{\partial y} = \frac{\partial N_\alpha}{\partial y}\alpha_{61}^e$$

$$\frac{\partial \tilde{v}}{\partial x} = \frac{\partial N_\alpha}{\partial x}\alpha_{62}^e, \quad \frac{\partial \tilde{v}}{\partial y} = \frac{\partial N_\alpha}{\partial y}\alpha_{52}^e \tag{27}$$

Hence, the following equation may be written:

$$\mathbf{J}_{\tilde{\mathbf{u}},\mathbf{x}} = \mathbf{J}_{\tilde{\mathbf{u}},\xi}\mathbf{J}_{\xi,\mathbf{x}} = \begin{bmatrix} \dfrac{\partial \tilde{u}}{\partial \xi} & \dfrac{\partial \tilde{u}}{\partial \eta} \\ \dfrac{\partial \tilde{v}}{\partial \xi} & \dfrac{\partial \tilde{v}}{\partial \eta} \end{bmatrix} \mathbf{J}_{\mathbf{x},\xi}^{-1} \tag{28}$$

or

$$\mathbf{J}_{\tilde{\mathbf{u}},\mathbf{x}} = -2\left(\begin{bmatrix} \xi(1-\eta^2) & 0 \\ 0 & 0 \end{bmatrix}\alpha_{51}^e + \begin{bmatrix} 0 & 0 \\ 0 & \eta(1-\xi^2) \end{bmatrix}\alpha_{52}^e + \begin{bmatrix} 0 & \eta(1-\xi^2) \\ 0 & 0 \end{bmatrix}\alpha_{61}^e + \begin{bmatrix} 0 & 0 \\ \xi(1-\eta^2) & 0 \end{bmatrix}\alpha_{62}^e \right)\mathbf{J}_{\mathbf{x},\xi}^{-1} \tag{29}$$

The strain field at the element level is defined by

$$\varepsilon = \varepsilon_d + \tilde{\varepsilon}_\alpha = [B_d^e \;\; \tilde{B}_\alpha^e] \begin{bmatrix} d^e \\ \alpha^e \end{bmatrix} \tag{30}$$

with

$$\tilde{\mathbf{B}}_\alpha^e = \begin{bmatrix} \dfrac{\partial N_\alpha}{\partial x} & 0 & 0 & 0 \\ 0 & \dfrac{\partial N_\alpha}{\partial y} & 0 & 0 \\ 0 & 0 & \dfrac{\partial N_\alpha}{\partial y} & \dfrac{\partial N_\alpha}{\partial x} \end{bmatrix} \tag{31}$$

The extra variables are eliminated in the assembling process by a substructuring technique, as in the enhanced assumed strain method.[15]

It is noteworthy that the constant nominal stress field condition referred above is satisfied due to the fact that:

$$\int_{\Omega} \tilde{\mathbf{B}}_{\alpha}^{e} \, \mathrm{d}\Omega = \int_{-1}^{1} \int_{-1}^{1} \tilde{\mathbf{B}}_{\alpha}^{e} \, j \, \mathrm{d}\xi \, \mathrm{d}\eta = \mathbf{0} \tag{32}$$

5. ELEMENTS ASSESSEMENT

In this section the performance of the elements proposed is assessed, especially near to the incompressible limit and comparisons are made with other elements referred above, in particular with:

(a) the Q4—standard bilinear element;
(b) the SRI—the previous element with reduced integration on the volumetric terms;
(c) the QM6—incompatible modes element,[10] equivalent to the assumed strain element of Simo and Rifai,[15] the original Q1/E4;
(d) the **B**-bar0—**B**-bar formulation,[7] with an approach that generalizes the selective reduced integration;
(e) the **B**-bar—**B**-bar formulation,[7] with an approach that generalizes the mean-dilatation formulation.

5.1. Beam bending

In this standard test,[7] the beam represented in Figure 7(a) is subjected to the following boundary conditions:

Displacement:

$$u(0, 0) = v(0, 0) = 0 \tag{33}$$

$$u(0, \pm c) = 0 \tag{34}$$

Traction:

$$\sigma_{yy}(x, \pm c) = \tau_{xy}(x, \pm c) = 0, x \in]0, L[\tag{35}$$

$$\left.\begin{aligned} \sigma_{xx}(L, y) &= 0 \\ \tau_{xy}(L, y) &= \frac{3}{4c^3}(c^2 - y^2) \end{aligned}\right\} y \in]-c, +c[\tag{36}$$

$$\left.\begin{aligned} \sigma_{xx}(0, y) &= -\frac{3L}{2c^3} y \\ \tau_{xy}(0, y) &= \frac{3}{4c^3}(c^2 - y^2) \end{aligned}\right\} y \in]-c, 0[\cup]0, +c[\tag{37}$$

The traction boundary conditions are those encountered in simple bending theory for a cantilever beam.

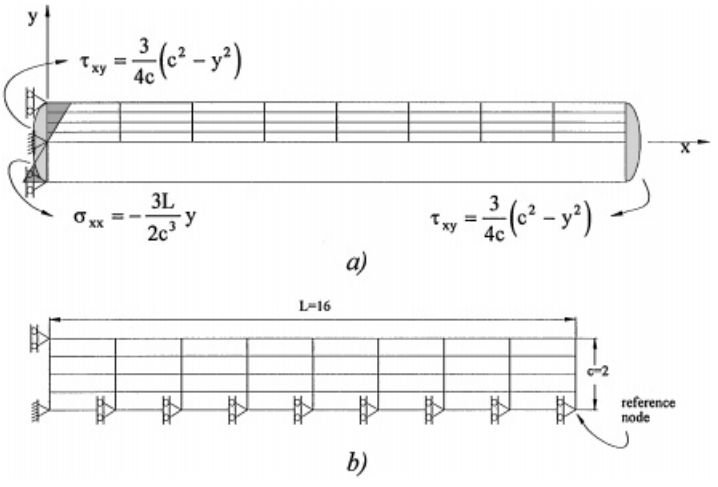

Figure 7. Finite element model for the beam bending problem

Only half of the domain is modelled due to anti-symmetry conditions and the mesh used is depicted in Figure 7(b). Plane strain conditions were assumed.

The analytical solution for the vertical displacement is

$$v(x, y) = \frac{(1-\upsilon^2)}{4Ec^3}\left(3\frac{\upsilon}{1-\upsilon}y^2(L-x) + c^2x\left(4 + 5\frac{\upsilon}{1-\upsilon}\right) + 3x^2\left(L - \frac{1}{3}x\right)\right) \tag{38}$$

in which E is the Young's modulus and υ is the Poisson's ratio and for the reference node (see Figure 7(b)) we have

$$v(16,0) = \frac{(1-\upsilon^2)L^3}{2Ec^3}\left(\frac{c^2}{2L^2}\left(4 + 5\frac{\upsilon}{1-\upsilon}\right) + 1\right) \tag{39}$$

To normalize the results the Young's modulus may be defined as a function of the Poisson's ratio to give for the tip vertical displacement the value $v(16,0) = 1$ as

$$E(\upsilon) = \frac{(1-\upsilon^2)L^3}{2c^3}\left(\frac{c^2}{2L^2}\left(4 + 5\frac{\upsilon}{1-\upsilon}\right) + 1\right) \tag{40}$$

The ratio of the Lamé parameters:

$$\frac{\lambda}{\mu} = \frac{\upsilon}{2(1-2\upsilon)} \tag{41}$$

tends to infinity as the Poisson's ratio approaches 0·5. In Figure 8 the behaviour on this situation is compared for different elements.

As it may be seen, the performance of the standard four-node element is very poor. The incompatible modes element, the proposed Qi5 and Qi6 elements, the SRI element and the **B**-bar

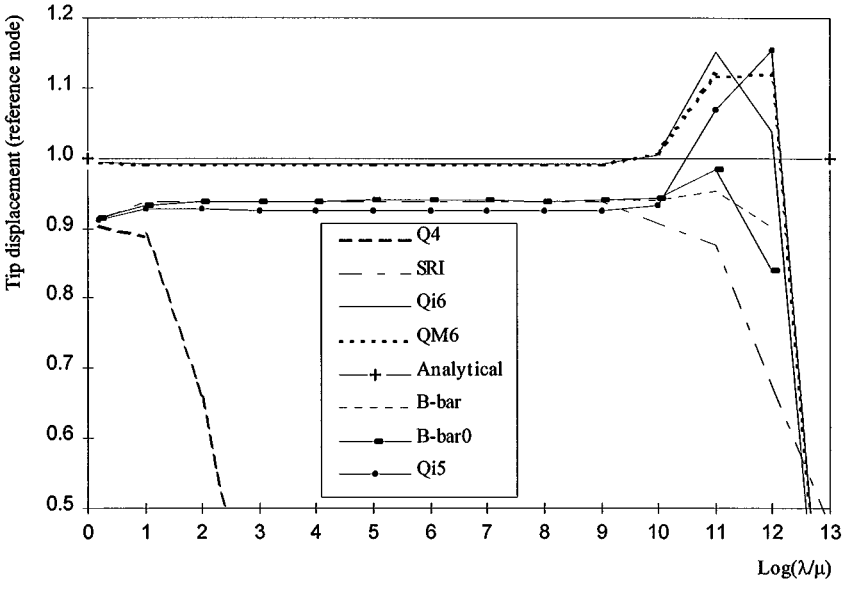

Figure 8. Vertical displacement of the reference node

approaches maintain their accuracy even for large ratios of λ/μ. The Qi6 and QM6 elements have a similar performance, with excellent results, particularly for $\lambda/\mu \leqslant 10^{10}$.

5.2. *Cook's membrane*

In this example a clamped tapered panel is subjected to an in-plane shearing load using several mesh configurations.[26] This problem is usually utilized to ascertain good coarse mesh accuracy in bending problems and insensitivity to mesh distortion exhibited by different proposed elements (Figure 9).

The problem is solved assuming linear elasticity for two different values for the Poisson's ratio near to the incompressible limit. The simulation is performed under plane strain conditions and the values of the material constants for elastic cases are

$$E = 240{\cdot}565; \quad \upsilon = 0{\cdot}4999 \quad or \quad \upsilon = 0{\cdot}4999999$$

The vertical displacement of the top edge node is plotted against different mesh configurations for all the elements proposed, **B**-bar formulations and QM6 element in Figures 10 and 11.

For $\upsilon = 0{\cdot}4999$ all formulations appear to converge to the same answer, and meshes with more than 20×20 elements give for all formulations a similar result. However the **B**-bar, selective reduced integration approaches and the Qi5 element, require finer meshes.

For $\upsilon = 0{\cdot}4999999$ only the SRI, the Qi5, the Qi6 and the **B**-bar appear to converge to the same answer. Furthermore, only these formulations show a completely insensitivity to mesh distortion. However, and with 20×20 elements all formulations have the same result although the **B**-bar approaches require much finer meshes.

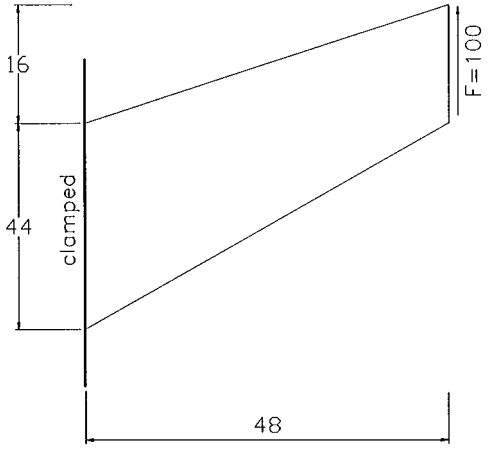

Figure 9. Cook's membrane problem

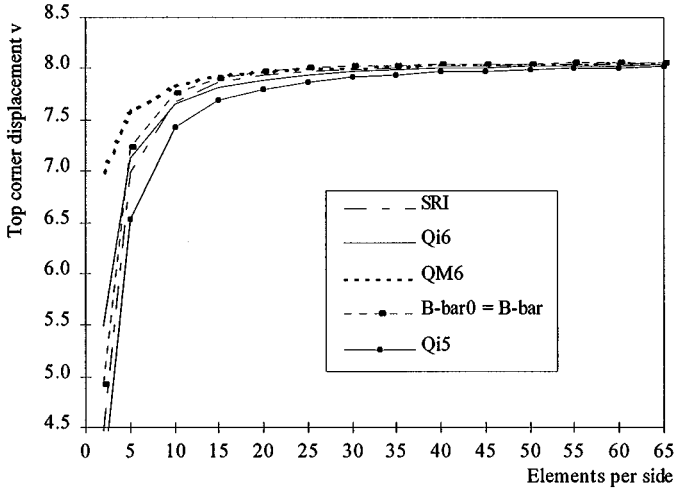

Figure 10. Displacement of Cook's membrane problem ($\upsilon = 0{\cdot}4999$)

5.3. *Extension of a double edge notched specimen*

This test was introduced by Nategaal *et al.*[4] to demonstrate the spurious response of standard displacement models in highly constrained plane strain elastoplastic problems. A perfect plastic von Mises model is assumed, and the values of the material constants are taken as

$$\sigma_y = 0{\cdot}243, \quad E = 70, \quad \upsilon = 0{\cdot}3$$

where σ_y is the uniaxial yield stress.

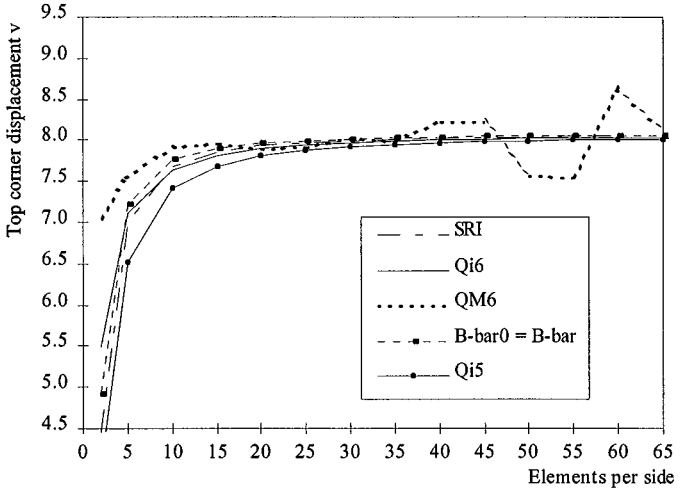

Figure 11. Displacement of Cook's membrane problem ($\upsilon = 0{\cdot}4999999$)

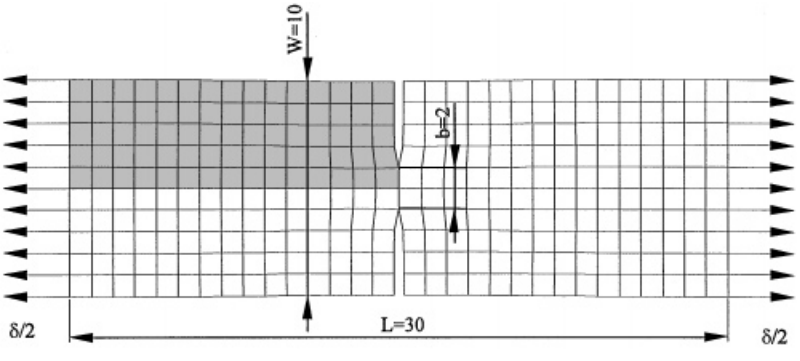

Figure 12. Double edge notched tension specimen

The simulation is carried out by displacement controlled load steps at the left side of the specimen. A 5×15 mesh (Figure 12) is used to model a quarter of the problem using symmetry boundary conditions. Each displacement step corresponds to:

$$\Delta\delta = \frac{1}{2}\frac{\sigma_y W}{E}$$

In Figure 13 the total extensional load versus the normalized horizontal deflection ($E\delta/\sigma_y W$), where δ is the displacement at the left side (30 time steps), is represented.

It is clear, the convergence of Qi6, QM6, Qi5 and SRI to the analytical solution, while the Q4 exhibits locking.

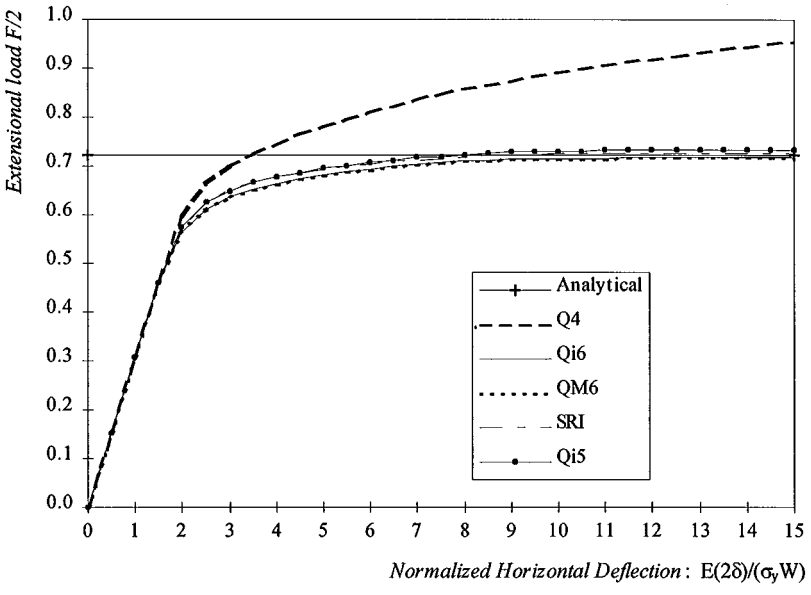

Figure 13. The load-deflection plots of double edge notched tension

5.4. *Locking problem*

In this example, we try to reproduce the locking test of Section 3 using a 2×2 finite element mesh and examine the performance of the Qi6 and the QM6 elements when some element distortion is imposed (Figure 14).

5.4.1. Dislocation of the central node. In this case, the central node position is changed causing the distortion of the mesh. In Figure 15, for a Poisson's ratio of $\upsilon = 0{\cdot}3$, the errors of the displacement of nodes 1 and 9, relatively to those obtained with a regular mesh are represented. The proposed Qi6 element shows a better performance in this compressible situation.

For near incompressible situations the same errors on nodes 1 and 9 are represented in Figure 16. In Figure 17 the values obtained for the displacement of node 7, which is zero for a regular mesh, are shown. The proposed Qi6 element has a much better performance on near incompressible situations than the QM6.

5.4.2. Rotation about the central node. In this example the mesh is distorted by rotating the interior sides of the elements about the central node. For a near incompressible situation Figure 18 shows the variation on the displacement of node 7, which should be zero, for different values of the rotation angle. The proposed Qi6 element gives the correct value whilst the QM6 element shows a very poor performance. In Figure 19, for the same situation the error on the displacement of node 1 is represented. Again, it is evident the better performance of the proposed Qi6 element.

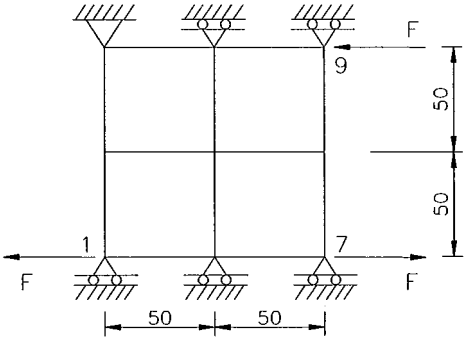

Figure 14. Finite element model for the locking test

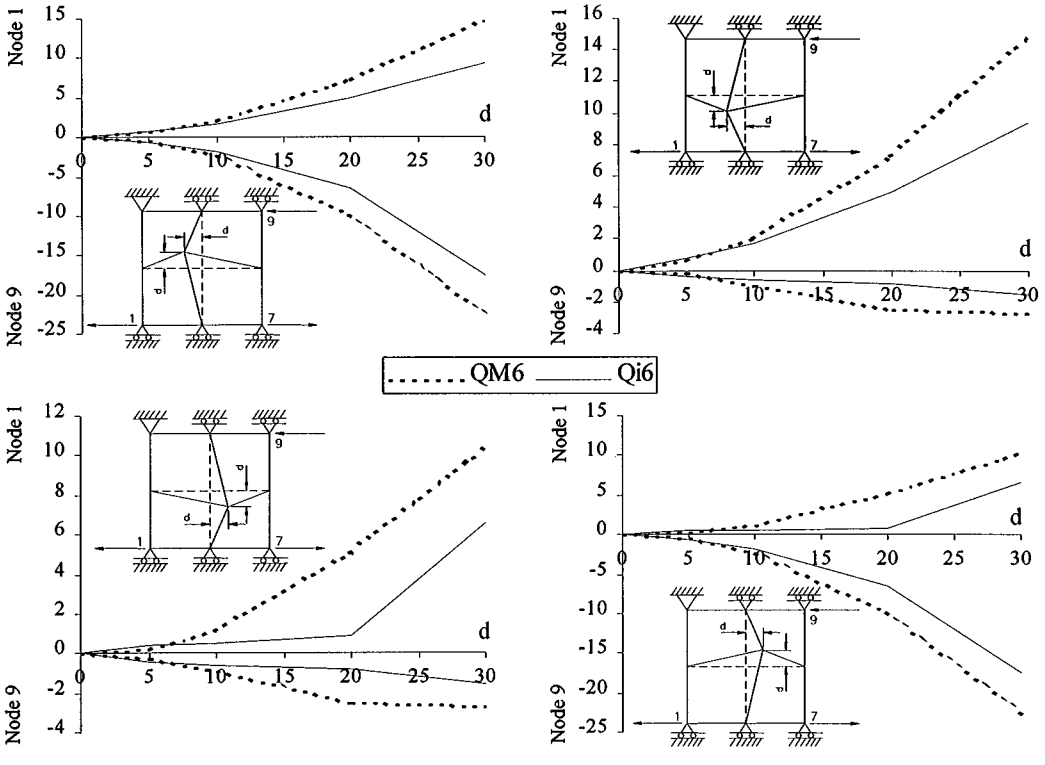

Figure 15. Error on nodes 1 and 9 with $\upsilon = 0{\cdot}3$

6. CONCLUSIONS

Two new elements were proposed. The Qi5 was designed with the same methodology of the incompatible modes element but is based on compatible modes and has only two extra degrees of

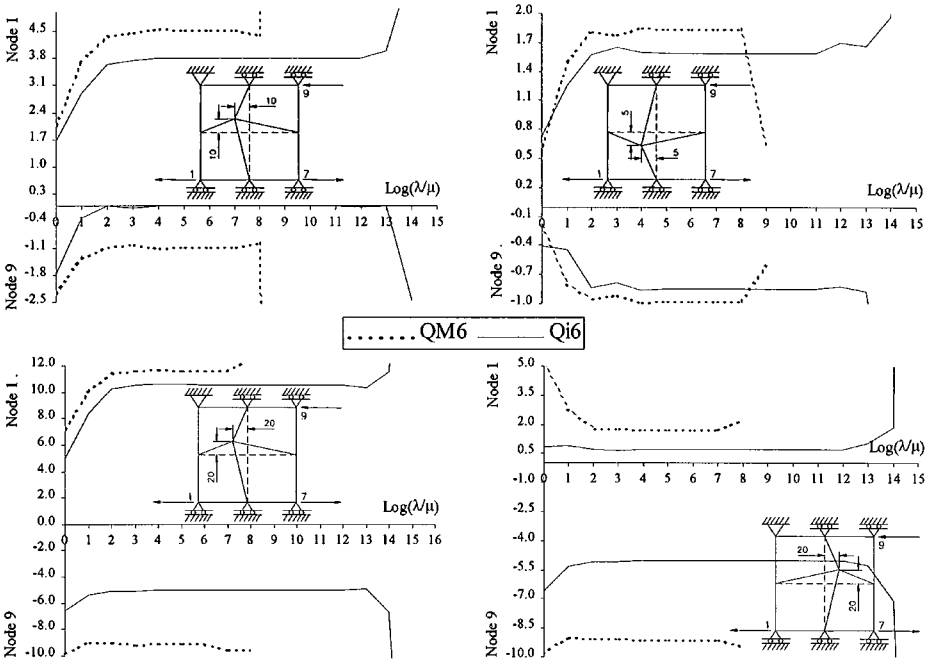

Figure 16. Error on nodes 1 and 9

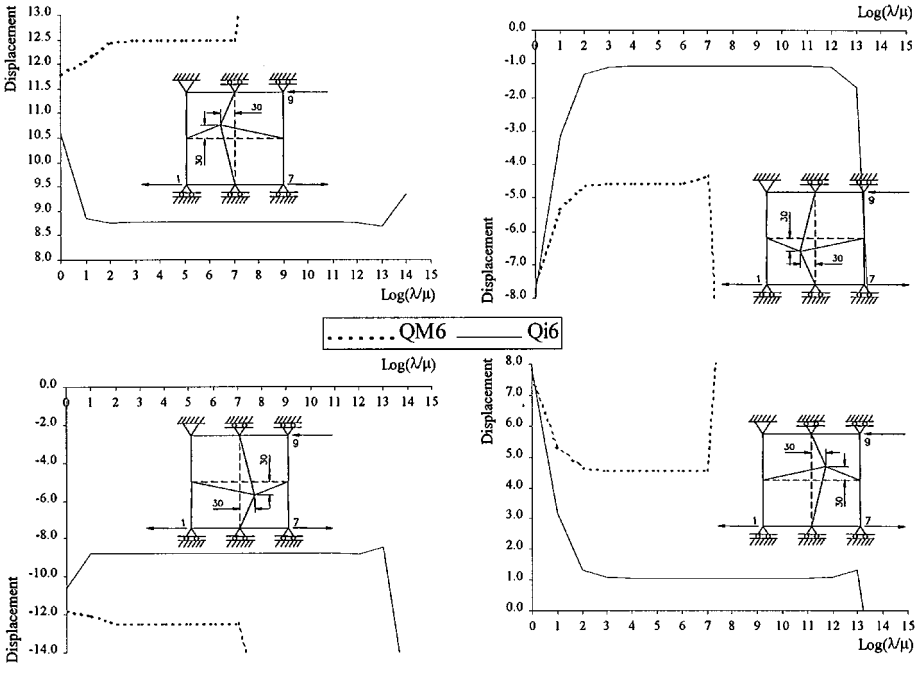

Figure 17. Displacement of node 7

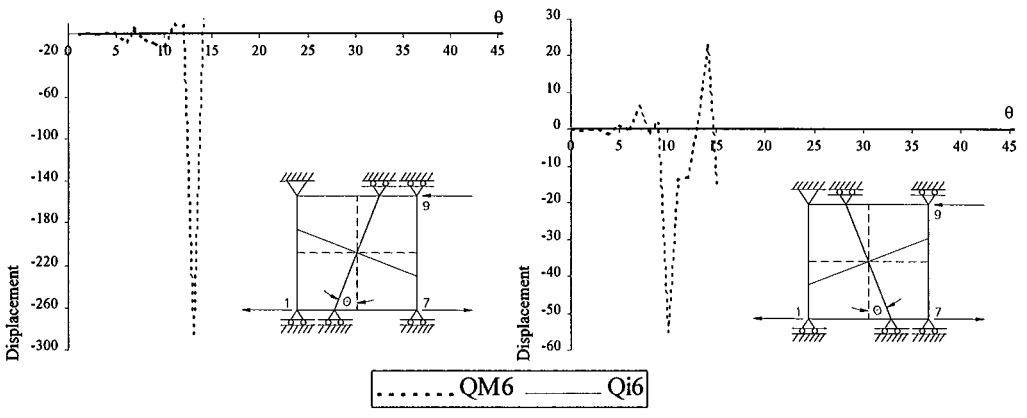

Figure 18. Displacement on node 7 with $\mathrm{Log}(\lambda/\mu) = 9$

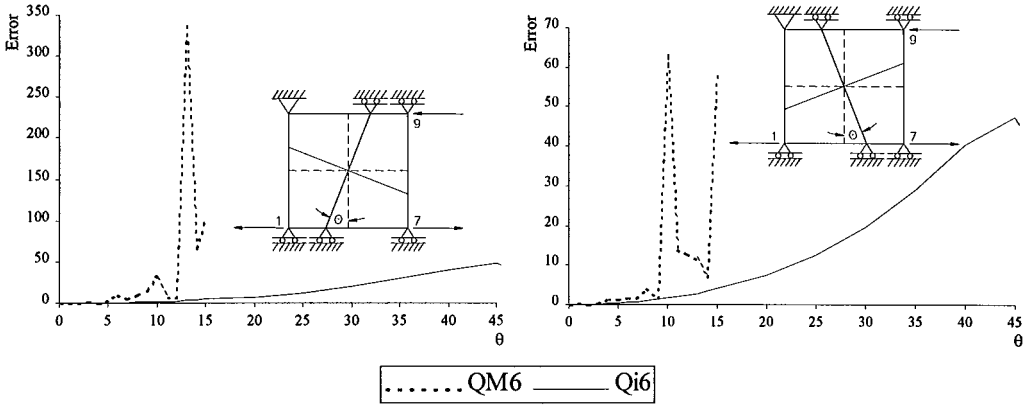

Figure 19. Error on node 1 with $\mathrm{Log}(\lambda/\mu) = 9$

freedom. The Qi6 was designed following a similar methodology to the enhanced strain mixed method. These elements showed a good performance in different incompressible situations and in particular the Qi6 element is more accurate than the original enhanced strain element in distorted meshes.

The elements proposed have only been tested in geometrically linear problems. The generalization of the ideas behind the implementation of these elements into the large strain field will be the next step of this work.

ACKNOWLEDGEMENT

The financial support of Programa PRAXIS XXI do Ministério da Ciência e Tecnologia e do FEDER through the Project 3/3.1/CEG/2643/95 is gratefully aknowledged.

REFERENCES

1. D. J. Naylor, 'Stresses in nearly incompressible materials for the finite elements with the application to the calculation of excess pore pressures', *Int. J. Numer. Meth. Engng*., **8,** 443–460 (1974).
2. J. C. Nagtegaal, D. M. Parks and J. R. Rice, 'On numerically accurate finite element solutions in the fully plastic range', *Comput. Meth. Appl. Mech. Engng*., **4,** 153–178 (1974).
3. O. C. Zienkiewicz and P. N. Godbole, 'Viscous incompressible flow with special reference to non-Newtonian (plastic) flows', in R. H. Gallagher *et al.* (eds.), *Finite Elements in Fluids*, Vol. 1, Wiley Chichester, 1975.
4. T. J. R. Hughes, R. L. Taylor and J. F. Levy, 'High Reynolds number, steady, incompressible flows by a finite element method', in R. H. Gallagher *et al.* (eds.), *Finite Elements in Fluids*, Vol. 3, Wiley Chichester, 1978.
5. D. S. Malkus and T. J. R. Hughes, 'Mixed finite element methods-reduced and selective integration techniques: a unification of concepts', *Comput. Meth. Appl. Mech. Engng*., **15,** 63–18 (1978).
6. T. J. R. Hughes, 'Generalisation of selective integration procedures to anisotropic and nonlinear media', *Int. J. Numer. Meth. Engng*., **15,** 1413–1418 (1980).
7. T. J. R. Hughes, *The Finite Element Method-Linear Static and Dynamic Finite Element Analysis*, Prentice-Hall International Inc., Englewood Cliffs, N.J., 1987.
8. O. C. Zienkiewicz and R. L. Taylor, *The Finite Element Method*, Vol.1, McGraw-Hill, New York, 1989.
9. E. L. Wilson, R. L. Taylor, W. P. Doherty and J. Ghaboussi, 'Incompatible displacement models', *in* S. J. Fenves, N. Perrone, A. R. Robinson and W. C. Schnobrich (eds.), *Numerical and Computer Models in Structural Mechanics*, Academic Press, New York, 1973, pp. 43–57.
10. R. L. Taylor, P. J. Beresford and E. L. Wilson, 'A non-conforming element for stress analysis', *Int. J. Numer. Meth. Engng*., **10,** 1211–1219 (1976).
11. D. Kosloff and G. A. Frazier, 'Treatment of hourglass pattern in low order finite element codes', *Int. J. Num. Analyt. Meth. Geomech*., **2,** 57–72 (1972).
12. T. Belytschko and W. E. Bachrach, 'Efficient implementation of quadrilaterals with high coarse-mesh accuracy', *Comput. Meth. Appl. Mech. Engng*., **54,** 279–301 (1986).
13. J. M. A. César de Sá, 'Numerical modelling of incompressible problems in glass forming and rubber technology', *Ph.D. Thesis*, University College of Swansea, C/Ph/91/86, U.K., 1986.
14. J. M. A. César de Sá. and D. R. J. Owen, 'The imposition of the incompressibility constraint in finite elements—A review of methods with a new insight to the locking phenomenon', in C. Taylor *et al.* (eds.), *Proc. 3rd Int. Conf. on Numerical Methods for Non-Linear Problems, Dubrovnik*, Pineridge Press Ltd., Swansea, U.K. 1986.
15. J. C. Simo and M. S. Rifai, 'A class of mixed assumed strain methods and the method of incompatible modes', *Int. J. Numer. Meth. Engng*., **29,** 1595–1638 (1990).
16. J. C. Simo and F. Armero, 'Geometrically non-linear enhanced strain mixed methods and the method of incompatible modes', *Int. J. Numer. Meth. Engng*., **33,** 1413–1449 (1992).
17. J. C. Simo, F. Armero and R. L. Taylor, 'Improved versions of assumed enhanced strain tri-linear elements for 3D finite deformation problems', *Comput. Meth. Appl. Mech. Engng*., **110,** 359–386 (1993).
18. M. A. Crisfield, G. F. Moita, G. Jelenic and L. P. R. Lyons, 'Enhanced lower-order element formulations for large strains', in D. R. J. Owen *et al.* (eds.), *Proc. 4th Int. Conf. on Computational Plasticity: Fundamentals and Applications, Barcelona*, Pineridge Press Ltd., Swansea, U.K., 1995, pp. 293–320.
19. K. Arunakirinathar and B. D. Reddy, 'Enhanced strain finite element methods', in D. R. J. Owen *et al.* (eds.), *Proc. 4th Int. Conf. on Computational Plasticity: Fundamentals and Applications, Barcelona*, Pineridge Press Ltd., Swansea, U.K., 1995, pp. 321–332.
20. M. Schonauer, E. A. de Souza Neto and D. R. J. Owen, 'Hencky tensor based enhanced large strain element for elasto-plastic analysis', in D. R. J. Owen *et al.* (eds.), *Proc. 4th Int. Conf. on Computational Plasticity: Fundamentals and Applications, Barcelona*, Pineridge Press Ltd., Swansea, U.K., 1995, pp. 333–348.
21. E. A. de Souza Neto, D. Peric, G. C. Huang and D. R. J. Owen, 'Remarks on the stability of enhanced strain elements in finite elasticity and elastoplasticity', in D. R. J. Owen *et al.* (eds.), *Proc. 4th Int. Conf. on Computational Plasticity: Fundamentals and Applications, Barcelona*, Pineridge Press Ltd., Swansea, U.K., 1995, pp. 361–372.
22. E. A. de Souza Neto, D. Peric, M. Dutko and D. R. J. Owen, 'Design of simple low order finite elements for large strain analysis of nearly incompressible solids', *Int. J. Solids Struct*., **33,** 3277–3296 (1996).
23. U. Hueck and P. Wriggers, 'A formulation for the 4-noded quadrilateral element', *Int. J. Numer. Meth. Engng*., **38,** 3007–3037 (1995).
24. P. Wriggers and U. Hueck, 'A formulation for the QS6 element for large elastic deformations', *Int. J. Numer. Meth. Engng*., **39,** 1437–1454 (1996).
25. E. N. Dvorkin and S. I. Vassolo, 'A quadrilateral 2-D finite element based on mixed interpolation of tensorial components', *Engng. Comput*., **6,** 217–224 (1989).
26. R. D. Cook, D. S. Malkus and M. E. Plesha, *Concepts and Applications of Finite Element Analysis*, Wiley, New York, 1989.

